

QoE-driven Secure Video Transmission in Cloud-edge Collaborative Networks

Tantan Zhao, Lijun He, Xinyu Huang, Fan Li*

Abstract—Video transmission over the backhaul link in cloud-edge collaborative networks usually suffers security risks. Only a few existing studies focus on ensuring secure backhaul link transmission. However, video content characteristics, which have significant effects on quality of experience (QoE), are ignored in the study. In this paper, we investigate the QoE-driven cross-layer optimization of secure video transmission over the backhaul link in cloud-edge collaborative networks. First, we establish the secure transmission model for backhaul link by considering video encoding and MEC-caching in a distributed cache scenario. Then, based on the established model, a joint optimization problem is formulated with the objective of improving user QoE and reducing transmission latency under the constraints of MEC capacity. To solve the optimization problem, we propose two algorithms: a near optimal iterative algorithm based on relaxation and branch and bound method (MC-VEB), and a greedy algorithm with low computational complexity (Greedy MC-VEB). Simulation results show that our proposed MC-VEB can greatly improve the user QoE and reduce transmission latency within security constraints, and the proposed Greedy MC-VEB can obtain the tradeoff between the user QoE and the computational complexity.

Index Terms—QoE, cross-layer optimization, backhaul link security, MEC-caching, video encoding.

I. INTRODUCTION

With the rapid development of video processing technology and mobile communication technology, large numbers of ultra-high-definition (UHD) video-on-demand (VoD) facing massive links have emerged. The number of user video requests is growing dramatically, leading to the heavy traffic load of networks and high latency of users. These factors could bring poor QoE for video-requesting users. Luckily, mobile edge computing (MEC) technology, as one of the key technologies of the cloud-edge collaboration networks in the fifth generation(5G) system, provides a promising method to handle these challenges [1], [2]. Since MEC servers are closer to the users at the network edge and own powerful intelligent storage capabilities to precache hot videos, massive video contents can be delivered directly to users from MEC servers to reduce backhaul traffic burden [3] and transmission latency. Therefore, how to utilize MEC to meet the high QoE requirements of video users is worth studying.

Manuscript received December 23, 2024. This work was supported in part by the National Science Foundation of China under Grant 62071369 and in part by the Key Research and Development Program of Shaanxi Province under Grant 2020KW-009..

T. Zhao, L. He, X. Huang and F. Li are with the School of Information and Communications Engineering, Xi'an Jiaotong University, Xi'an 710049, China (e-mail: {zhao10111446, xinyu_huang}@stu.xjtu.edu.cn; {lijunhe, lifan}@mail.xjtu.edu.cn). (Corresponding author: Fan Li, email: lifan@mail.xjtu.edu.cn)

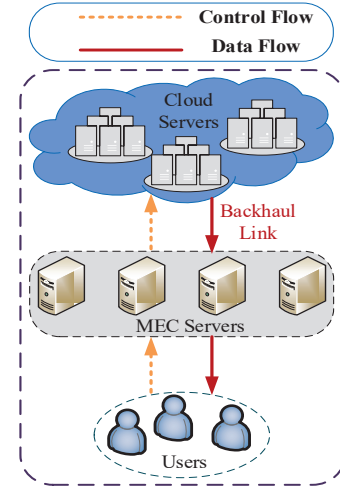


Fig. 1. Transmission Architecture in Cloud-edge Collaborative Networks.

In recent years, the copyright protection of video is becoming more and more important. Moreover, the emerging paid VIPs and confidential data services that only specific users can receive make the secure transmission of video contents into an issue that cannot be ignored in the cloud-edge collaborative networks.

To be specific, for the video transmission in the cloud-edge collaborative networks, when the video data is transmitted from the cloud server to the user in unicast mode, the eavesdropping user and the legitimate user receive information on the same frequency channel at the same time. Once the channel condition of the eavesdropper is better than that of the legitimate user, the eavesdropper could successfully intercept the video packets, which causes data leakage and infringes on the video copyright and the benefits of the users. Therefore, the secure data transmission is important. For the transmission security of the link from the MEC server to the users, as depicted in Fig. 1, the existing physical layer secure (PLS) mechanism, which has been studied intensively and extensively, is sufficient. [4]–[7]. However, the PLS mechanism is complicated and high-cost because it could ensure the security of each video packet. If it is utilized to ensure the transmission security of the backhaul link from the cloud server to the MEC server, as depicted in Fig. 1, the traffic load of the backhaul link is so heavy that the cost and system overhead could be unbearable in the distributed cache scenario, where an MEC server may be connected to multiple base stations. Therefore,

it is an urgent issue to develop a secure mechanism with low complexity and cost to ensure the secure transmission of the backhaul link from the cloud to the MEC server, rather than using the strict and complicated traditional PLS mechanism.

In recent years, the issue of the secure backhaul link in the cloud-edge collaborative networks is rarely considered. Only the authors in [33] considered the security risks of the backhaul link when studying the optimal cache placement in edge heterogeneous networks. Nevertheless, the issue aimed at general data transmission, ignoring the characteristics of the video applications, which resulted in the poor performance for video transmission applications. Therefore, secure video transmission through the backhaul links in the cloud-edge collaborative networks is still an open question.

To address the abovementioned problems in secure video transmission through backhaul links in cloud-edge collaborative networks, we propose a QoE-driven cross-layer optimization algorithm to improve the user QoE, reduce transmission latency and guarantee the security of the backhaul links. The main contributions of this paper can be summarized as follows.

- 1) *Establishing a Video Encoding and MEC Caching-based Secure Transmission Model*: Video encoding and MEC caching act together in ensuring secure transmission of backhaul links. However, the existing secure transmission model for backhaul links completely ignores this important characteristic of video encoding. The lack of flexible adjustable features of video encoding parameters leads to the secure transmission for backhaul links not being able to be guaranteed when the caching capacity of MEC servers is limited. Based on this issue, we comprehensively consider the interaction of video encoding parameters and MEC caching strategy and establish video encoding and a secure MEC caching-based transmission model for backhaul links.
- 2) *Formulating Joint Optimization Problem of Video Encoding and MEC Caching*: Different from general data services, the fundamental goal of video services is to improve user QoE. Based on the established secure transmission model for backhaul links, we incorporate video encoding and MEC caching into the same mathematical model and formulate a joint optimization problem of video encoding parameters and MEC caching strategy to improve user QoE, reduce transmission latency and prevent video information leakage.
- 3) *Proposing Near Optimal and Suboptimal Solutions*: We propose a near-optimal algorithm based on relaxation and branch and bound to solve the formulated optimization problem, which is a nonlinear mixed 0-1 integer programming problem. To be specific, we first relax the original optimization problem into a nonlinear programming problem without integer constraints, then use the 0-1 branch and bound method to obtain the integer solution of the original optimization problem. Furthermore, considering that the near-optimal algorithm is time-consuming, we also propose a suboptimal algorithm based on the greedy method with low computational complexity to get the tradeoff between the user QoE and the computational complexity.

The rest of this paper is organized as follows. Section II reviews the related works. In Section III, we introduce the system model, which includes the framework of QoE-driven cross-layer system and describe the secure transmission model. In Section IV, we formulate the QoE maximization and latency minimization problem under the secure constraints. In Section V we propose a near optimal solution based on joint optimization of video encoding and MEC caching. In Section VI, we propose a suboptimal solution based on greedy method. Section VII gives the experimental results, and discusses the performance gains of the proposed algorithms compared to the existing algorithm. Finally, Section VIII concludes this paper.

II. RELATED WORK

In this section, we will review and analyze the progress of existing related work from the following two aspects.

A. QoE-driven MEC Video Caching

The MEC servers are closer to users and have powerful storage capabilities. By caching multimedia contents during off-peak hours, delay and congestion can be reduced, thereby improving mobile user QoE [8], [9].

To exploit the storage capacity of MEC servers, the authors in [10] proposed a distributed cache optimization algorithm through belief propagation of MEC heterogeneous networks, which greatly reduced the download delay of users. From the perspective of the basic information theoretical limit of MEC-caching, the authors in [11] gave the best trade-off between latency and caching. Considering the particularity of video transmission, the researchers in [12] proposed a co-caching strategy for small-cell base stations (SBSs) and mobile devices, which greatly reduced the delay in video content delivery.

In addition to latency, the popularity of video contents also determines whether the cached videos meet the needs of users. The authors in [13], [14] proposed a context-aware caching scheme to predict the popularity and learn the video popularity of a specific context online, which is used to determine the cache replacement strategy. However, with the increasing heterogeneity of user groups demanding specific video content, the issue of caching mobile video streaming has become a more complicated task. Therefore, there are also many papers that use machine learning to predict preferences of users [15]–[20].

The studies mentioned above are for traditional video streaming, to improve the QoE of dynamic adaptive streaming users. The authors in [21] studied the QoE-driven optimization of MEC-caching placement for dynamic adaptive video streaming, which considers the different rate-distortion characteristics of videos and the coordination among distributed MEC servers. The authors in [22] proposed a refined caching update strategy based on video popularity, content importance, and user playback status, which ensured that the video segments to be played by users could be cached in time. To further improve user QoE, multiple modules in addition to MEC -aching are considered to be optimized comprehensively. The authors in [23] proposed to enhance

the QoE-aware wireless edge caching with bandwidth provisioning in software-defined wireless networks. Specifically, a joint optimization mechanism of caching strategy, bandwidth configuration, and adaptive video streaming was designed to reduce delay and improve QoE. In addition, the researchers in [24] proposed a joint scheme of caching strategy, power allocation, user association, and adaptive video streaming to improve the system spectrum efficiency and user QoE, but this scheme will cause a greater burden on backhaul traffic. Therefore, in [25], the authors studied the joint optimization scheme of mobile terminal QoE and backhaul traffic, which reduced power consumption and backhaul traffic, meanwhile improving QoE. Although the above studies aim to improve the QoE of mobile users, security issues in the cloud-edge collaborative networks were not considered.

B. Caching-based Secure Transmission

With the increasing complexity of the network environment, legal transmission in the networks is inevitably attacked by external malicious nodes, or the SBS originally used for caching becomes a malicious node and implements eavesdropping. Therefore, the cache-based secure transmission scheme aroused the interest of researchers.

For the secure transmission of general wireless caching networks, the authors in [26] studied the security of caching networks from the perspective of information theory by using the network coding, while the authors in [27] considered the security of device-to-device caching networks. Based on the previous studies, in [28], the authors studied the secure device-to-device coding and caching scheme in the sense of information theory, and the authors in [29] proposed a decentralized secure coding caching method in wireless ad hoc networks. However, all above studies focus on wireless physical layer security, which is ensured by the complicated PLS mechanism with high cost.

For the secure transmission of the mobile edge heterogeneous cache network, the researchers in [30] studied the attack models in MEC systems and proposed a security solution based on reinforcement learning techniques for the mobile edge caching. The authors in [31] proposed a secure caching solution for disaster backup in mobile social networks using fog computing, and the authors in [32] proposed a secure caching solution in heterogeneous multihoming edge computing networks. However, all the above studies are about the secure transmission problem of the attacked cache server itself and ignore the security risks of backhaul links.

Apart from the above studies, for the security risks of backhaul links, the authors in [33] studied the optimal cache placement problem under secrecy constraints of backhaul links in edge heterogeneous networks. Specifically, the authors proposed an MEC-caching strategy to minimize the average backhaul link rate and ensure the security of backhaul links. However, what has been studied in this study is a secure transmission scheme for general data, which ignored the unique characteristics of videos, i.e., different encoding parameters correspond to different encoding rates which bring different QoEs. Therefore, the proposed secure scheme is not specific to video transmission services.

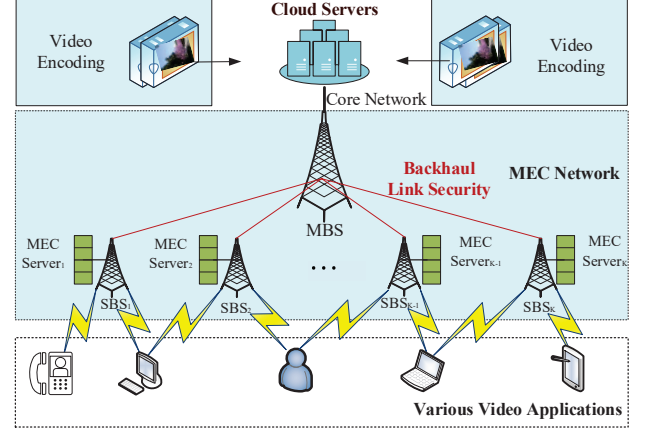


Fig. 2. VoD Downlink Transmission in Cloud-edge Collaborative Networks.

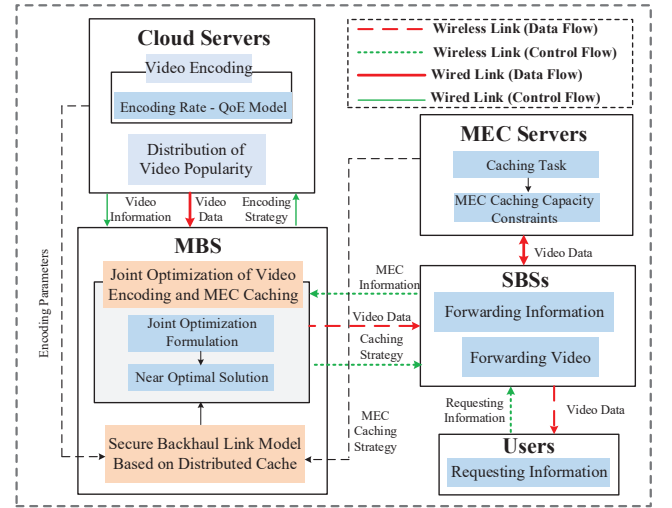


Fig. 3. QoE-driven Joint Optimization Scheme of Video Encoding and MEC Caching Based on Secure Backhaul Link Model.

III. SYSTEM MODEL

A. Framework

In this paper, we consider a VoD downlink scenario in the cloud-edge collaborative networks, where multiple users request video files from the cloud servers via a macro-cell base station (MBS), which has access to the cloud servers through wired core network. SBSs are deployed in the coverage area of the MBS to serve user video requests, as depicted in Fig. 2. The number of MEC servers is K , and let \mathcal{K} denote the set of K MEC servers and the caching capacity of each MEC is $\Phi_k, \forall k \in \mathcal{K}$. Each MEC is connected to an SBS. A user requesting video files is initially served by SBSs. For video services without packet loss, n encoding packets are required to successfully decode video information. If the number of video packets sent by all MEC servers within the connection range is m and less than n , the decoding conditions are not met. Then, the MBS is contacted to send the remaining $n - m$ video packets to the user via backhaul link.

Based on the above scenario, we propose a QoE-driven joint optimization scheme of video encoding and MEC-caching based on the secure transmission model for the backhaul link, as illustrated in Fig. 3.

Specifically, the whole block diagram of the joint optimization scheme contains the modules of MBS, cloud servers, SBSs, MEC servers and users. First, the video encoding information, i.e., encoding rate, QoE model and the distribution of popularity, from the cloud servers, and the MEC information, i.e., the caching capacity and the number of MEC servers from the SBSs are sent to the system analysis module MBS. Then, the optimal encoding and caching strategy based on the collected information and the secure transmission model of backhaul link are designed by the MBS and sent to the cloud servers and the SBSs, respectively. The secure transmission model of the backhaul link is video encoding and MEC-caching-based, which means that the encoding packet size, the number of encoding packets cached in the MEC servers and the capacity of MEC servers together determine whether the secure transmission can be achieved. Finally, the video streamings are encoded by the cloud servers according to the designed encoding strategy and cached in the MEC servers according to the designed caching strategy after being transmitted from the cloud servers. Different from the eavesdropping which comes from the wireless physical layer, here we consider utilizing the adjustable encoding parameters and the distributed MEC cache to avoid data leakage in the backhaul links from the MBS to the SBSs and construct the secure transmission model of backhaul links. Based on the secure transmission model, the QoE-driven joint optimization model of video encoding and MEC caching is established.

B. Video Encoding and MEC Caching-based Secure Transmission Model

For the high-definition (HD)/UHD VoD services, we assume that there are F original video streamings to be encoded and cached, and let \mathcal{F} denote the set of F video streamings. $p_j, \forall j \in \mathcal{F}$ indicates the requesting probability of a user for the j -th video file, which is ranked in descending order of video popularity. Without loss of generality, we can mark the most popular video file with index 1 and the lowest popular video file with index F . Specifically, the requesting probability of a user for a video file can be described as a Zipf distribution. Assuming that all video files are sorted according to their popularity, the probability of being requested for each video file can be obtained by the following formula:

$$p_j = \frac{1/j^{-\theta}}{\sum_{j=1}^F 1/j^{-\theta}}, 0 < \theta < 1, \forall j \in \mathcal{F} \quad (1)$$

where θ is the tilt factor of the distribution, which is used to control the distribution of video popularity, and the larger value means more concentrated probability of video requests.

Specifically, the following assumptions are made when encoding and caching video streamings:

- 1) Each video file is encoded into n packets of different sizes, and let \mathcal{N} denote the set of n encoding packets.

Let $s_{i,j}$ denote the size of the i -th video packet of the j -th video file. The n video encoding packets are cached distributedly in different MEC servers.

- 2) $\tilde{m}_{k,i,j}$ denotes whether the i -th video packet of the j -th video file is cached in the k -th MEC server ($\tilde{m}_{k,i,j} = 1$) or not ($\tilde{m}_{k,i,j} = 0$).

Based on the above assumptions, the caching strategy of MEC servers can be formulated as a matrix $\mathbf{M}_{K \times F}$ of size $K \times F$, where the rows indicate the MEC servers, the columns indicate the video files, and the element $m_{k,j}$ represents the number of video encoding packets of the j -th video file cached in the k -th MEC server, obviously, $m_{k,j} = \sum_{i=1}^n \tilde{m}_{k,i,j}$. Specifically, the matrix $\mathbf{M}_{K \times F}$ can be expressed as the following form:

$$\mathbf{M}_{K \times F} = \begin{bmatrix} m_{11} & \cdots & m_{1F} \\ \vdots & \ddots & \vdots \\ m_{K1} & \cdots & m_{KF} \end{bmatrix} \quad (2)$$

As a result, for each request, the number of video packets of the j -th video file that need to be transmitted through the backhaul links can be expressed as

$$R_j = n - \min \left(n, \sum_{k=1}^K m_{kj} \right) \quad (3)$$

Meanwhile, assuming that the number of total requests during the whole delivery phase received by SBSs is Ψ , then the number of requests for the video file j received by SBSs is $\Psi_j = \Psi \cdot p_j, \forall j \in \mathcal{F}$. Therefore, for Ψ_j requests, the total number of encoding packets for the j -th video file transmitted through the backhaul links can be obtained as follows

$$P_j = \Psi_j \cdot \left[n - \min \left(n, \sum_{k=1}^K m_{kj} \right) \right] \quad (4)$$

For clarity, considering that $n \geq \sum_{k=1}^K m_{kj}$ in our considered scenario, Eq. (4) can be further formulated as

$$P_j = \Psi_j \cdot \left(n - \sum_{k=1}^K m_{kj} \right) \quad (5)$$

We know that for the video services without packet loss, secure transmission can be realized if and only if $P_j \leq n - 1$. Consequently, the secure transmission model of backhaul link based on the distributed MEC cache can be expressed by

$$\Psi_j \cdot \left(n - \sum_{k=1}^K m_{kj} \right) \leq n - 1 \quad (6)$$

After further simplification, we can get

$$\sum_{k=1}^K m_{kj} \geq n \cdot \left(1 - \frac{1}{\Psi_j} \right) + \frac{1}{\Psi_j} \quad (7)$$

Based on the above derivation, we know that the probability of secure transmission for the requested video is closely related to the encoding packets cached in each MEC server and the number of video requests.

IV. PROBLEM FORMULATION

Based on the secure transmission model achieved for backhaul links, the QoE-driven joint optimization problem of video encoding parameters and MEC-caching strategy under the constraints of MEC capacity and video encoding rate has been formulated. We define the optimization variables as $\tilde{\mathbf{M}}_{K \times n \times F} = \{\tilde{m}_{k,i,j}, \forall k \in \mathcal{K}; \forall i \in \mathcal{N}; \forall j \in \mathcal{F}\}$ and $\mathbf{S}_{n \times F} = \{s_{i,j}, \forall i \in \mathcal{N}; \forall j \in \mathcal{F}\}$, where $\tilde{m}_{k,i,j}$ and $s_{i,j}$ denote the caching strategy and the size of each video encoding packet, respectively. To improve user QoE, we construct the joint optimization problem expressed by Eq. (8) as follows:

$$\begin{aligned}
 & \max_{\tilde{\mathbf{M}}, \mathbf{S}} Q(\tilde{\mathbf{M}}, \mathbf{S}) \\
 & \text{s.t.} \\
 & (c1) \tilde{m}_{k,i,j} \in \{0, 1\}, \forall k \in \mathcal{K}; \forall i \in \mathcal{N}; \forall j \in \mathcal{F} \\
 & (c2) \sum_{j=1}^F \sum_{i=1}^n \tilde{m}_{k,i,j} s_{i,j} \leq \Phi_k, \forall k \in \mathcal{K} \\
 & (c3) \sum_{k=1}^K \sum_{i=1}^n \tilde{m}_{k,i,j} \leq n, \forall j \in \mathcal{F} \\
 & (c4) \sum_{k=1}^K \sum_{i=1}^n \tilde{m}_{k,i,j} \geq n \cdot \left(1 - \frac{1}{\Psi_j}\right) + \frac{1}{\Psi_j}, \forall j \in \mathcal{F} \\
 & (c5) R_{\min_j} \leq \frac{\sum_{i=1}^n s_{i,j}}{T_d} \leq R_{\max_j}, \forall j \in \mathcal{F}
 \end{aligned} \tag{8}$$

where $Q(\cdot)$ is the objective function for different application demands, which can represent a single optimization objective or the combination of multiple optimization objectives, depending on the practical application demands. $R_{\min_j}, \forall j \in \mathcal{F}$ and $R_{\max_j}, \forall j \in \mathcal{F}$ denote the maximum and minimum encoding rates of the j -th video file, and the larger encoding rate means the higher QoE. T_d denotes the duration of each video file.

Specifically, in our considered VoD downlink scenario, the optimization objective is to maximize the QoE and minimize the transmission latency at the same time. Then, the $Q(\cdot)$ can be defined as

$$Q(\tilde{\mathbf{M}}, \mathbf{S}) = \sum_{j=1}^F [f(s_{i,j}) - g(\tilde{m}_{k,i,j}, s_{i,j})], \tag{9}$$

where $f(s_{i,j})$ denotes the relationship between the size of the video encoding packets and QoE, which is determined by the chosen QoE model, and $g(\tilde{m}_{k,i,j}, s_{i,j})$ denotes the relationship among the caching strategy, the size of video encoding packets and the transmission latency. In particular, according to the MOS model in [34], for the j -th video file, $f(s_{i,j})$ and $g(\tilde{m}_{k,i,j}, s_{i,j})$ can be expressed as

$$f(s_{i,j}) = C_{1j} \cdot \left(\frac{\sum_{i=1}^n s_{i,j}}{T_d}\right)^3 + C_{2j} \cdot \left(\frac{\sum_{i=1}^n s_{i,j}}{T_d}\right)^2 + C_{3j} \cdot \left(\frac{\sum_{i=1}^n s_{i,j}}{T_d}\right) + C_{4j} \tag{10}$$

where $C_{1j}, C_{2j}, C_{3j}, C_{4j}, \forall j \in \mathcal{F}$ are QoE parameters which can be determined by the range of the video encoding rate of the j -th video file for a given MOS model.

$$g(\tilde{m}_{k,i,j}, s_{i,j}) = V_j \cdot \left[\frac{p_j \cdot \left(\sum_{i=1}^n s_{i,j} - \sum_{i=1}^n \sum_{k=1}^K \tilde{m}_{k,i,j} s_{i,j} \right)}{R_{bk}} \right]^{\frac{2}{3}} \tag{11}$$

where $V_j, \forall j \in \mathcal{F}$ is the weighting coefficient of transmission latency for a given MOS model. R_{bk} is the transmission rate of the backhaul link.

Constraint (c1) indicates whether the k -th MEC server caches the i -th packet of the j -th video file or not. Constraint (c2) indicates that the sum of video packet sizes cached in each MEC server should not be greater than the MEC capacity $\Phi_k, \forall k \in \mathcal{K}$. Constraint (c3) indicates the number of video encoding packets cached in all MEC servers should not be larger than the total number of video encoding packets n . Constraint (c4) reveals the number of video encoding packets that need to be cached in MEC servers to ensure the secure transmission of backhaul links. Constraint (c5) gives the maximum and the minimum limits of encoding rate for each video streaming.

V. NEAR OPTIMAL SOLUTION BASED ON JOINT OPTIMIZATION OF VIDEO ENCODING AND MEC CACHING

The optimization problem formulated in section IV can be observed to be a nonlinear mixed integer programming problem, which means that a part of the decision variables must be integers, called integer-variables, while others can be nonintegers, called noninteger variables. To solve it, a near-optimal solution based on relaxation and branch and bound method is proposed in this subsection. Specifically, the whole solving procedure can be divided into two steps, i.e., relaxation of the original nonlinear mixed 0-1 integer problem and the near-optimal solution based on the 0-1 branch and bound method. In the following section of this paper, we will describe them in detail.

A. Relaxation of the Original Nonlinear Mixed 0-1 Integer Problem

For the mixed integer programming problem, the classical idea of solving the problem is to relax the original mixed integer programming problem with integer constraints into the relaxing problem without integer constraints and obtain the solution of the original mixed integer programming problem based on the solution of its relaxing problem. Therefore, we can easily get the relaxing problem, which can be expressed by the following:

$$\begin{aligned}
 & \max_{\tilde{\mathbf{M}}, \mathbf{S}} \sum_{j=1}^F [f(s_{i,j}) - g(\tilde{m}_{k,i,j}, s_{i,j})] \\
 & \text{s.t.} \\
 & (c1) \sum_{j=1}^F \sum_{i=1}^n \tilde{m}_{k,i,j} s_{i,j} \leq \Phi_k, \forall k \in \mathcal{K} \\
 & (c2) \sum_{k=1}^K \sum_{i=1}^n \tilde{m}_{k,i,j} \leq n, \forall j \in \mathcal{F} \\
 & (c3) \sum_{k=1}^K \sum_{i=1}^n \tilde{m}_{k,i,j} \geq n \cdot \left(1 - \frac{1}{\Psi_j}\right) + \frac{1}{\Psi_j}, \forall j \in \mathcal{F} \\
 & (c4) R_{\min_j} \leq \frac{\sum_{i=1}^n s_{i,j}}{T_d} \leq R_{\max_j}, \forall j \in \mathcal{F}
 \end{aligned} \tag{12}$$

Particularly, the relaxing processing is based on the fact that the optimal solution of the mixed integer programming, denoted as $\tilde{\mathbf{M}}_{opt}$ and \mathbf{S}_{opt} , will not be superior to the optimal solution of its relaxing problem, which is the upper bound of the original mixed integer programming. Here, the definition

of the relaxing problem can be expressed as: the objective function and remaining constraints of the original mixed integer programming problem without considering the integer constraints.

The relaxing problem (12) above is a maximization problem, which is obtained by removing the first integer constraint (c1) in the original mixed 0-1 integer programming problem (8). For this maximization problem, as a typical reformulation method for optimization programming, we consider a minimization problem equivalent to the maximization problem (12) as follows

$$\begin{aligned}
& \min_{\tilde{\mathbf{M}}, \mathbf{S}} \sum_{j=1}^F [g(\tilde{m}_{k,i,j}, s_{i,j}) - f(s_{i,j})] \\
& \text{s.t.} \\
& (c1) \sum_{j=1}^F \sum_{i=1}^n \tilde{m}_{k,i,j} s_{i,j} \leq \Phi_k, \forall k \in \mathcal{K} \\
& (c2) \sum_{k=1}^K \sum_{i=1}^n \tilde{m}_{k,i,j} \leq n, \forall j \in \mathcal{F} \\
& (c3) \sum_{k=1}^K \sum_{i=1}^n \tilde{m}_{k,i,j} \geq n \cdot \left(1 - \frac{1}{\Psi_j}\right) + \frac{1}{\Psi_j}, \forall j \in \mathcal{F} \\
& (c4) R_{\min_j} \leq \frac{\sum_{i=1}^n s_{i,j}}{T_d} \leq R_{\max_j}, \forall j \in \mathcal{F}
\end{aligned} \tag{13}$$

The minimization problem (13) is actually a nonlinear optimization problem. Therefore, we consider utilizing the global optimal algorithm GlobalSearch provided by Global Optimization Toolbox of MATLAB to obtain its solution. Actually, the near-optimal solution of the optimization problem (13) can be obtained by the use of the GlobalSearch algorithm, which is a kind of heuristic search algorithm. Here, we can denote the near optimal solution of the relaxing problem (13) as $\tilde{\mathbf{M}}_r$ and \mathbf{S}_r , and the corresponding objective function value is Q_r .

B. Near Optimal Solution based on 0-1 Branch and Bound

To obtain the optimal solution of the original mixed integer programming, we employ the branch and bound method [35]. Specifically, we can discuss the solution of the relaxing problem (13) in two cases.

In case one, the solution in $\tilde{\mathbf{M}}_r$ concerning integer-variables $\tilde{\mathbf{M}}_{K \times n \times F} = \{\tilde{m}_{k,i,j}, \forall k \in \mathcal{K}; \forall i \in \mathcal{N}; \forall j \in \mathcal{F}\}$ are integers. Then, the optimal solution $\tilde{\mathbf{M}}_r$ and \mathbf{S}_r of the relaxing problem is also the optimal solution of the original nonlinear mixed optimization problem and the optimal solution is obtained as $\mathbf{M}_{opt} = \tilde{\mathbf{M}}_r$, $\mathbf{S}_{opt} = \mathbf{S}_r$.

In case two, an element of solution $\tilde{\mathbf{M}}_r$ concerning integer-variables $\tilde{\mathbf{M}}_{K \times n \times F} = \{\tilde{m}_{k,i,j}, \forall k \in \mathcal{K}; \forall i \in \mathcal{N}; \forall j \in \mathcal{F}\}$ is not integer. Then, the solution should be branched. The whole procedure of branching can be divided into the following three steps.

- *Equality Constraints of 0 and 1 Branches Acquirement*

The optimal solution $\tilde{\mathbf{M}}_{opt}$ can be initialized as $\tilde{\mathbf{M}}_{opt} = \tilde{\mathbf{M}}_r$. Without loss of generality, in our nonlinear mixed integer optimization problem to be solved, we use $\tilde{m}_{k',i',j'}, \forall k' \in \mathcal{K}; \forall i' \in \mathcal{N}; \forall j' \in \mathcal{F}$ to denote the integer-variable which does not satisfy the integer constraint and $b_{k',i',j'}, \forall k' \in \mathcal{K}; \forall i' \in \mathcal{N}; \forall j' \in \mathcal{F}$ to denote its corresponding noninteger solution. Specifically, branch means that the relaxing

problem (13) obtained from the original nonlinear mixed integer problem should be further relaxed into two new sub-relaxing-problems, which can be named sub-relaxing-problem one and sub-relaxing-problem two. Relaxing means adding two inequality constraints concerning integer-variable $\tilde{m}_{k',i',j'}, \forall k' \in \mathcal{K}; \forall i' \in \mathcal{N}; \forall j' \in \mathcal{F}$ to the relaxing problem (13) and keeping its original objective function and remaining constraints. Specifically, for the sub-relaxing-problem one, the added inequality constraint can be expressed as $\tilde{m}_{k',i',j'} \leq \lfloor b_{k',i',j'} \rfloor, \forall k' \in \mathcal{K}; \forall i' \in \mathcal{N}; \forall j' \in \mathcal{F}$, while for the sub-relaxing-problem two, the added inequality constraint is $\tilde{m}_{k',i',j'} \geq \lfloor b_{k',i',j'} \rfloor + 1, \forall k' \in \mathcal{K}; \forall i' \in \mathcal{N}; \forall j' \in \mathcal{F}$, where $\lfloor \cdot \rfloor$ means rounding down.

Particularly, in our original nonlinear mixed integer optimization problem (8), each indicative variable $\tilde{m}_{k,i,j}, \forall k \in \mathcal{K}, \forall i \in \mathcal{N}, \forall j \in \mathcal{F}$ of the caching strategy has only two possible values, namely, 0 or 1. As a result, the considered nonlinear mixed integer optimization problem (8) is actually a nonlinear mixed 0-1 integer programming problem.

Meanwhile, considering that 0-1 integer programming is the special case of the general integer programming problem, the idea of solving 0-1 integer programming is actually to add a lower bound and an upper bound constraint to each integer-variable based on general integer programming. Therefore, from the characteristics of the branch and bound method and 0-1 integer programming problem, the inequality constraints here in the two sub-relaxing-problems can be simplified into the equality constraints. Specifically, the inequality constraint $\tilde{m}_{k',i',j'} \leq \lfloor b_{k',i',j'} \rfloor, \forall k' \in \mathcal{K}; \forall i' \in \mathcal{N}; \forall j' \in \mathcal{F}$ in the sub-relaxing-problem one can be equivalently transformed into equality constraint $\tilde{m}_{k',i',j'} = 0, \forall k' \in \mathcal{K}; \forall i' \in \mathcal{N}; \forall j' \in \mathcal{F}$ and the inequality constraint $\tilde{m}_{k',i',j'} \geq \lfloor b_{k',i',j'} \rfloor + 1, \forall k' \in \mathcal{K}; \forall i' \in \mathcal{N}; \forall j' \in \mathcal{F}$ in the sub-relaxing-problem, the two can be equivalently transformed into the equality constraint $\tilde{m}_{k',i',j'} = 1, \forall k' \in \mathcal{K}; \forall i' \in \mathcal{N}; \forall j' \in \mathcal{F}$. In this situation, we can rename the general branch and bound method as the 0-1 branch and bound method employed in our nonlinear mixed 0-1 integer programming problem.

- *Two Sub-relaxing-problems Formulation*

Based on the obtained minimization relaxing problem (13) and equality constraints of the 0-1 branch, we can easily get the sub-relaxing-problem one and sub-relaxing-problem two as follows:

Sub-relaxing-problem one:

$$\begin{aligned}
& \min_{\tilde{\mathbf{M}}, \mathbf{S}} \sum_{j=1}^F [g(\tilde{m}_{k,i,j}, s_{i,j}) - f(s_{i,j})] \\
& \text{s.t.} \\
& (c1) \sum_{j=1}^F \sum_{i=1}^n \tilde{m}_{k,i,j} s_{i,j} \leq \Phi_k, \forall k \in \mathcal{K} \\
& (c2) \sum_{k=1}^K \sum_{i=1}^n \tilde{m}_{k,i,j} \leq n, \forall j \in \mathcal{F} \\
& (c3) \sum_{k=1}^K \sum_{i=1}^n \tilde{m}_{k,i,j} \geq n \cdot \left(1 - \frac{1}{\Psi_j}\right) + \frac{1}{\Psi_j}, \forall j \in \mathcal{F} \\
& (c4) R_{\min_j} \leq \frac{\sum_{i=1}^n s_{i,j}}{T_d} \leq R_{\max_j}, \forall j \in \mathcal{F} \\
& (c5) \tilde{m}_{k',i',j'} = 0, \forall k' \in \mathcal{K}; \forall i' \in \mathcal{N}; \forall j' \in \mathcal{F}
\end{aligned} \tag{14}$$

where constraint (c5) represents the 0 branch of the integer-variable $\tilde{m}_{k',i',j'}, \forall k' \in \mathcal{K}; \forall i' \in \mathcal{N}; \forall j' \in \mathcal{F}$.

Sub-relaxing-problem two:

$$\begin{aligned}
& \min_{\tilde{\mathbf{M}}, \mathbf{S}} \sum_{j=1}^F [g(\tilde{m}_{k,i,j}, s_{i,j}) - f(s_{i,j})] \\
& \text{s.t.} \\
& (c1) \sum_{j=1}^F \sum_{i=1}^n \tilde{m}_{k,i,j} s_{i,j} \leq \Phi_k, \forall k \in \mathcal{K} \\
& (c2) \sum_{k=1}^K \sum_{i=1}^n \tilde{m}_{k,i,j} \leq n, \forall j \in \mathcal{F} \\
& (c3) \sum_{k=1}^K \sum_{i=1}^n \tilde{m}_{k,i,j} \geq n \cdot \left(1 - \frac{1}{\Psi_j}\right) + \frac{1}{\Psi_j}, \forall j \in \mathcal{F} \\
& (c4) R_{\min,j} \leq \frac{\sum_{i=1}^n s_{i,j}}{T_d} \leq R_{\max,j}, \forall j \in \mathcal{F} \\
& (c5) \tilde{m}_{k',i',j'} = 1, \forall k' \in \mathcal{K}; \forall i' \in \mathcal{N}; \forall j' \in \mathcal{F}
\end{aligned} \tag{15}$$

where constraint (c5) represents the 1-branch of the integer-variable $\tilde{m}_{k',i',j'}, \forall k' \in \mathcal{K}; \forall i' \in \mathcal{N}; \forall j' \in \mathcal{F}$.

The remaining constraints (c1) to (c4) in sub-relaxing-problem one (14) and sub-relaxing-problem two (15) are the constraints in the minimization relaxing problem (13), and the objective function is the objective function in the minimization relaxing problem (13).

• Near Optimal Solution Obtainment

The sub-relaxing-problem one formulated in Eq. (14) and the sub-relaxing-problem two formulated in Eq. (15) can also be solved by the GlobalSearch algorithm due to their forms similar to the minimization relaxing problem (13).

There are only two possible solution for the two sub-relaxing-problems expressed by Eq. (14) and Eq. (15), i.e., infeasible solution or integer solution, due to the equivalent transformation of inequality constraints into equality constraints when considering the 0-1 branch and bound method. For the convenience of solving the problem, if the infeasible solution appears for the sub-relaxing-problem, we can directly set it as positive infinity or negative infinity, which depends on whether the relaxing problem is a maximization problem or a minimization problem. Then, the optimal solution for one iteration of 0-1 branch and bound can be obtained by comparing the objective function values of the two sub-relaxing-problems to find the minimization branch and its corresponding solution, denoted as $\tilde{\mathbf{M}}_{\min}$ and \mathbf{S}_{\min} , which are used to update the optimal solution $\tilde{\mathbf{M}}_{\text{opt}}$ and \mathbf{S}_{opt} for each iteration by letting $\tilde{\mathbf{M}}_{\text{opt}} = \tilde{\mathbf{M}}_{\min}$ and $\mathbf{S}_{\text{opt}} = \mathbf{S}_{\min}$.

A new noninteger solution may appear in the updated solution $\tilde{\mathbf{M}}_{\text{opt}}$ due to the 0-1 branch and bound. Therefore, if there is still one noninteger solution in the obtained $\tilde{\mathbf{M}}_{\text{opt}}$, the 0-1 branch and bound should be executed continually based on the sub-relaxing-problems formulated in Eq. (14) and Eq. (15). Specifically, 0 and 1 constraints concerning the new noninteger solution should be added to the sub-relaxing-problems (14) and (15). Then, the optimal solution $\tilde{\mathbf{M}}_{\text{opt}}$ and \mathbf{S}_{opt} can be obtained by updating them as the optimal solution of the minimization branch of the current iteration of 0-1 branch and bound. Finally, the optimal solution of the original nonlinear mixed integer optimization problem can be obtained until there is no noninteger solution in the updated optimal solution $\tilde{\mathbf{M}}_{\text{opt}}$. The corresponding objective function value Q_{\min} can be obtained by substituting the near optimal solution

$\tilde{\mathbf{M}}_{\text{opt}}$ and \mathbf{S}_{opt} into the objective function of the optimization problem (13).

Generally speaking, to obtain the near-optimal integer solution of the considered optimization problem formulated in Eq. (13), the maximum iteration to execute 0-1 branch and bound is $K \cdot n \cdot F$, which is actually the number of elements in the three-dimensional integer variable $\tilde{\mathbf{M}}_{K \times n \times F} = \{\tilde{m}_{k,i,j}, \forall k \in \mathcal{K}; \forall i \in \mathcal{N}; \forall j \in \mathcal{F}\}$. Particularly, for each iteration of the 0-1 branch and bound, if there is more than one noninteger element, denoted as $N_n, N_n \geq 2$, in the updated solution $\tilde{\mathbf{M}}_{\text{opt}}$, 0-1 branch and bound should be executed for each noninteger solution. Then, $2 \cdot N_n$ branches are generated, which are compared to find the minimization branch and its corresponding solution $\tilde{\mathbf{M}}_{\min}$ and \mathbf{S}_{\min} to update the optimal solution as $\tilde{\mathbf{M}}_{\text{opt}} = \tilde{\mathbf{M}}_{\min}$, $\mathbf{S}_{\text{opt}} = \mathbf{S}_{\min}$.

The solving procedure of our proposed near-optimal algorithm is summarized in Algorithm 1 named Near Optimal Algorithm Based on Relaxation and Branch and Bound Method.

VI. SUBOPTIMAL SOLUTION BASED ON GREEDY METHOD

Considering that the near-optimal algorithm proposed above is time-consuming, we propose a greedy algorithm with low computational complexity to obtain the sub-optimal solution of the original nonlinear mixed 0-1 integer programming problem.

The main idea of the greedy algorithm is to optimize variables $\tilde{\mathbf{M}} = \{\tilde{m}_{k,i,j}, \forall k \in \mathcal{K}; \forall i \in \mathcal{N}; \forall j \in \mathcal{F}\}$ and $\mathbf{S} = \{s_{i,j}, \forall i \in \mathcal{N}; \forall j \in \mathcal{F}\}$ separately. The whole procedure is presented in the following two subsections.

A. Caching Strategy Optimization with Encoding Parameters Fixed

First, we optimize variable $\tilde{\mathbf{M}}_{K \times n \times F} = \{\tilde{m}_{k,i,j}, \forall k \in \mathcal{K}; \forall i \in \mathcal{N}; \forall j \in \mathcal{F}\}$ with the encoding parameters fixed. The solution of variable $\tilde{\mathbf{M}}_{K \times n \times F} = \{\tilde{m}_{k,i,j}, \forall k \in \mathcal{K}; \forall i \in \mathcal{N}; \forall j \in \mathcal{F}\}$ can be obtained by solving the optimization problem (8) in the condition of giving the variable $\mathbf{S} = \{s_{i,j}, \forall i \in \mathcal{N}; \forall j \in \mathcal{F}\}$ a fixed value according to a given encoding rate. Actually, the solving process is the special case of Algorithm 1 with a fixed known \mathbf{S} , which greatly reduces the complexity of solving the optimization problem compared with a variable \mathbf{S} since the dimension of the optimization variable reduces.

According to Algorithm 1, with a fixed known \mathbf{S} , the optimization problem (13), (14) and (15) should be changed accordingly. Specifically, the minimization relaxing problem (13) can be reformulated as

$$\begin{aligned}
& \min_{\tilde{\mathbf{M}}} \sum_{j=1}^F g(\tilde{m}_{k,i,j}) \\
& \text{s.t.} \\
& (c1) \sum_{j=1}^F \sum_{i=1}^n \tilde{m}_{k,i,j} s_{i,j} \leq \Phi_k, \forall k \in \mathcal{K} \\
& (c2) \sum_{k=1}^K \sum_{i=1}^n \tilde{m}_{k,i,j} \leq n, \forall j \in \mathcal{F} \\
& (c3) \sum_{k=1}^K \sum_{i=1}^n \tilde{m}_{k,i,j} \geq n \cdot \left(1 - \frac{1}{\Psi_j}\right) + \frac{1}{\Psi_j}, \forall j \in \mathcal{F}
\end{aligned} \tag{16}$$

Algorithm 1 Near Optimal Algorithm Based on Relaxation and Branch and Bound Method

Input: $myfun1$: the objective function of optimization problem (13); $myfun2$: nonlinear constraints of optimization problem (13); linear constraints of optimization problem (13); $\tilde{\mathbf{M}}_0, \mathbf{S}_0$: initial solution of $\tilde{\mathbf{M}}$ and \mathbf{S} .

Output: $\tilde{\mathbf{M}}_{opt}, \mathbf{S}_{opt}$ and Q_{min} .

Initialize: Obtain $\tilde{\mathbf{M}}_r, \mathbf{S}_r$ and the objective function value Q_r by solving relaxing problem (13) utilizing the global optimal algorithm GlobalSearch. Calculate the initial total number of non-integer solution in $\tilde{\mathbf{M}}_r$, denoted as N_n , and obtain the corresponding position index vector \mathbf{N}_{in} . Initialize the left coefficient matrix of equality constraints (c5) of 0 branch in Eq. (14) and 1 branch in Eq. (15) as $\mathbf{A}_{eq} = \mathbf{0}$, and the corresponding right coefficient vector of equality constraints as $\mathbf{b}_{eq} = \mathbf{0}$.

if $N_n = 0$ **then**

$\tilde{\mathbf{M}}_{opt} = \tilde{\mathbf{M}}_r$;
 $\mathbf{S}_{opt} = \mathbf{S}_r$;
 $Q_{min} = Q_r$;

else

Initialize $\tilde{\mathbf{M}}_{opt} = \tilde{\mathbf{M}}_r$. Set the number of non-integer solution in $\tilde{\mathbf{M}}_{opt}$ for each iteration of 0-1 branch and bound as $N_b = N_n$ and the corresponding position index vector $\mathbf{N}_i = \mathbf{N}_{in}$.

for $p = 1$ **to** N_n **do**

for $q = 1$ **to** N_b **do**

Update $\mathbf{A}_{eq}(p, \mathbf{N}_i(:, q)) = 1$;
Obtain the left coefficient matrix of equality constraints for 0 and 1 branch $\mathbf{A}_{eq_zero} = \mathbf{A}_{eq}(1 : p, :)$, $\mathbf{A}_{eq_one} = \mathbf{A}_{eq}(1 : p, :)$;
Update $\mathbf{b}_{eq}(p, :) = 0$;
Obtain the right coefficient vector of equality constraints for 0 branch $\mathbf{b}_{eq_zero} = \mathbf{b}_{eq}(1 : p, :)$;
Update $\mathbf{b}_{eq}(p, :) = 1$;
Obtain the right coefficient vector of equality constraints $\mathbf{b}_{eq_one} = \mathbf{b}_{eq}(1 : p, :)$;
Solving the sub-relaxing-problem one (14) and the sub-relaxing-problem two (15) by utilizing the global optimal algorithm GlobalSearch.

end

Compare the objective function values of all 0-1 branches of N_b non-integer variables, and find the minimization branch and obtain its corresponding solution, denoted as $\tilde{\mathbf{M}}_{min}$ and \mathbf{S}_{min} ;

Update $\tilde{\mathbf{M}}_{opt}$ by setting $\tilde{\mathbf{M}}_{opt} = \tilde{\mathbf{M}}_{min}$, $\mathbf{S}_{opt} = \mathbf{S}_{min}$;

Update N_b and \mathbf{N}_i based on $\tilde{\mathbf{M}}_{opt}$.

end

Obtain $\tilde{\mathbf{M}}_{opt}, \mathbf{S}_{opt}$ and the objective function value Q_{min} by substituting $\tilde{\mathbf{M}}_{opt}$ and \mathbf{S}_{opt} into the objective function $myfun1$ of optimization problem (13).

end

Based on the reformulated minimization relaxing problem (16), the sub-relaxing-problem one (14) and sub-relaxing-problem two (15) can be reformulated as

Sub-relaxing-problem one:

$$\begin{aligned} & \min_{\tilde{\mathbf{M}}} \sum_{j=1}^F g(\tilde{m}_{k,i,j}) \\ & \text{s.t.} \\ & (c1) \sum_{j=1}^F \sum_{i=1}^n \tilde{m}_{k,i,j} s_{i,j} \leq \Phi_k, \forall k \in \mathcal{K} \\ & (c2) \sum_{k=1}^K \sum_{i=1}^n \tilde{m}_{k,i,j} \leq n, \forall j \in \mathcal{F} \\ & (c3) \sum_{k=1}^K \sum_{i=1}^n \tilde{m}_{k,i,j} \geq n \cdot \left(1 - \frac{1}{\Psi_j}\right) + \frac{1}{\Psi_j}, \forall j \in \mathcal{F} \\ & (c4) \tilde{m}_{k',i',j'} = 0, \forall k' \in \mathcal{K}; \forall i' \in \mathcal{N}; \forall j' \in \mathcal{F} \end{aligned} \quad (17)$$

where constraint (c4) represents the 0 branch of the integer-variable $\tilde{m}_{k',i',j'}, \forall k' \in \mathcal{K}; \forall i' \in \mathcal{N}; \forall j' \in \mathcal{F}$.

Sub-relaxing-problem two:

$$\begin{aligned} & \min_{\tilde{\mathbf{M}}} \sum_{j=1}^F g(\tilde{m}_{k,i,j}) \\ & \text{s.t.} \\ & (c1) \sum_{j=1}^F \sum_{i=1}^n \tilde{m}_{k,i,j} s_{i,j} \leq \Phi_k, \forall k \in \mathcal{K} \\ & (c2) \sum_{k=1}^K \sum_{i=1}^n \tilde{m}_{k,i,j} \leq n, \forall j \in \mathcal{F} \\ & (c3) \sum_{k=1}^K \sum_{i=1}^n \tilde{m}_{k,i,j} \geq n \cdot \left(1 - \frac{1}{\Psi_j}\right) + \frac{1}{\Psi_j}, \forall j \in \mathcal{F} \\ & (c4) \tilde{m}_{k',i',j'} = 1, \forall k' \in \mathcal{K}; \forall i' \in \mathcal{N}; \forall j' \in \mathcal{F} \end{aligned} \quad (18)$$

where constraint (c4) represents the 1 branch of the integer-variable $\tilde{m}_{k',i',j'}, \forall k' \in \mathcal{K}; \forall i' \in \mathcal{N}; \forall j' \in \mathcal{F}$.

B. Encoding Parameters Optimization Based on the Greedy Method

Then, based on the caching strategy $\tilde{\mathbf{M}}_g$ obtained, the solution of variable $\mathbf{S} = \{\tilde{s}_{i,j}, \forall i \in \mathcal{N}; \forall j \in \mathcal{F}\}$ can be obtained as \mathbf{S}_g by gradually increasing the encoding rate for each video file one by one in a certain reasonable step. In this way, we can find the one which brings the maximum MOS value of the current iteration until not meeting the constraints (c1) and (c4) of the optimization problem (13).

Finally, the suboptimal solution of the original nonlinear mixed noninteger solution can be obtained as $\tilde{\mathbf{M}}_g$ and \mathbf{S}_g . The corresponding objective function value Q_{min} can be obtained by substituting the suboptimal solution $\tilde{\mathbf{M}}_g$ and \mathbf{S}_g into the objective function of the optimization problem (13). The solving procedure for the greedy algorithm is summarized in Algorithm 2 named Greedy Algorithm based on Relaxation and Branch and Bound Method.

VII. SIMULATION RESULTS

In this section, we provide simulation results to highlight the performance of our algorithms. We consider a VoD downlink scenario in the cloud-edge network where the total number of video files is F , the total encoding packet of each video file is n , and the number of the MEC servers is K . The tilt factor of the Zipf distribution is assumed as $\theta = 0.8$. The duration of each video file is assumed as $T_d = 2400s$. The weighting coefficient of transmission latency is $V_j = 0.99, \forall j \in \mathcal{F}$. The

Algorithm 2 Greedy Algorithm Based on Relaxation and Branch and Bound Method

Input: Caching strategy \tilde{M}_g , which is obtained by utilizing Algorithm 1 with the known S based on the given encoding rate which satisfies constraint (c4) in optimization problem (13).

Output: \tilde{M}_g , S_g and Q_{min} .

Initialize: initialize S_g according to the minimum encoding rates of all video files; initialize Q_{min} as $Q_{min} = Q_g$ which is calculated based on the obtained \tilde{M}_g and S_g ; initialize increasing step of encoding rate as $\frac{1}{T_d \cdot n}$; initialize the searching times N_1 and N_2 as $N_1 = (R_{max} - R_{min}) \cdot T_d \cdot N$, $N_2 = F$, where N is the number of video files whose encoding rate lies between the minimum encoding rate R_{min} and the maximum encoding rate R_{max} .

for $p = 1$ **to** N_1 **do**

for $q = 1$ **to** N_2 **do**

 Obtain all possible S_g which satisfy constraints (c1) and (c4) in optimization problem (13) according to the increasing step $\frac{1}{T_d \cdot n}$.

 Obtain all possible Q_g by substituting all possible S_g , \tilde{M}_g into the objective function of optimization problem (13).

end

 Compare all possible Q_g and find the one which brings the most increments to Q_{min} , denoted as Q_{gmin} and its corresponding encoding parameters, denoted as S_{gmin} .

 Update S_g by setting $S_g = S_{gmin}$;

 Update Q_{min} by setting $Q_{min} = Q_{gmin}$.

end

transmission rate of the backhaul link is $R_{bk} = 10\text{Gbps}/F$. The total number of video requests received by SBSs during the whole delivery phase is ψ . In particular, we consider three types of video files, the encoding rates of which satisfy different encoding rate ranges:

Type 1: The encoding rates of the 1st to the $(2/F)$ -th video files vary from 0.3 Mbps to 0.7 Mbps;

Type 2: The encoding rates of the $(2/F+1)$ -th to the $(2/F+4/F)$ -th video files vary from 1Mbps to 4 Mbps;

Type 3: The encoding rates of the $(2/F+4/F+1)$ -th to the F -th video files vary from 4 Mbps to 8 Mbps.

The detailed parameter settings are presented in Table I. The secure issue of backhaul links in the cloud-edge collaborative networks is rarely considered, and only the authors in [33] studied the optimal cache placement in the condition of secure transmission of backhaul links. Therefore, our proposed schemes and the secure method in [33] are presented and analyzed:

- *MC-VEB*: Our proposed near-optimal MEC caching and video encoding-based (MC-VEB) algorithm includes video encoding parameters and an MEC-caching strategy that are jointly optimized.
- *Greedy MC-VEB*: Our proposed greedy MEC caching and video encoding-based (Greedy MC-VEB) algorithm with lower complexity compared with the near optimal

TABLE I
VIDEO FILE PARAMETERS

Types	Encoding rate range	QoE parameters
Type 1	0.3Mbps-0.7Mbps	$C_1 = 0.23, C_2 = -1.5,$ $C_3 = 3.3, C_4 = 2.5$
Type 2	1Mbps-4Mbps	$C_1 = 0.0426, C_2 = -0.4466,$ $C_3 = 1.6369, C_4 = 1.8415$
Type 3	4Mbps-8Mbps	$C_1 = 0.0027, C_2 = -0.0669,$ $C_3 = 0.5842, C_4 = 2.5248$

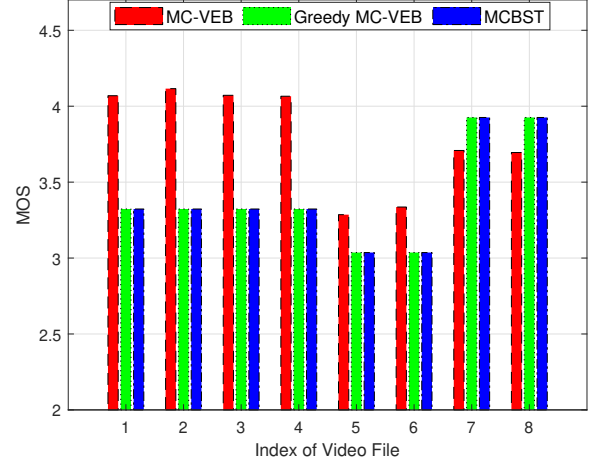


Fig. 4. MOS of each video file.

algorithm, includes video encoding parameters and an MEC caching strategy optimized step by step.

- *MCBST* in [33]: The MEC-caching-based secure transmission (MCBST) scheme, which aims to minimize the backhaul link rate under secrecy constraints by utilizing MEC caching strategy for general data transmission, does not consider adjusting encoding parameters for the video streaming.

We validate the algorithm performance in terms of MOS and average MOS with different simulation configurations.

A. MOS of Each Video File

Fig. 4 shows the MOS value of each video file with $n = 20$, $F = 8$, $K = 1$ and $\Phi_k = 26880\text{Mb}, \forall k \in \mathcal{K}$. Fig. 4 shows that, for each video file, the MOS performance of MC-VEB algorithm is not always superior to the MOS performance of the Greedy MC-VEB algorithm and MCBST scheme in spite of the obvious advantage in the average sense. The average MOS values of the MC-VEB algorithm, Greedy MC-VEB algorithm and MCBST scheme are 3.7935, 3.4021 and 3.4021, respectively, because our optimization goal is the whole performance advantage of all video files rather than the performance advantage for a single video file. Thus, there is no absolute superiority of MOS value for each video file in our proposed algorithm. Specifically, to obtain the whole performance advantage of the MOS value, the 1-st to 6-th video files, as depicted in Fig. 4, which can get higher QoE with lower encoding rate, are more likely to be distributed with caching capacity to improve QoE on the condition of limited

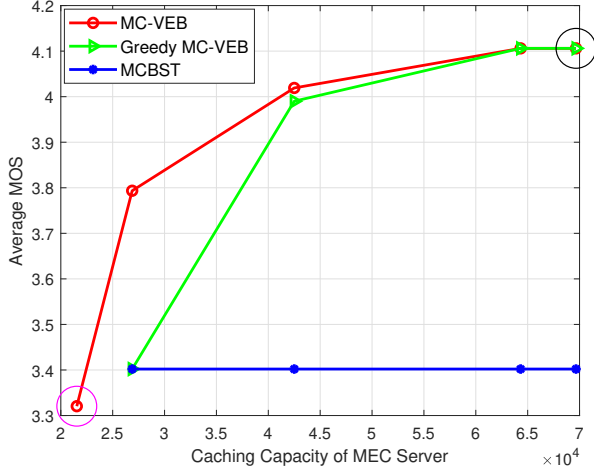


Fig. 5. Average MOS vs. different caching capacity of MEC server

caching capacity, while the 7-th and 8-th video files, which request higher encoding rate, are distributed with less caching capacity.

Each video file has a different caching strategy and encoding parameter. Therefore, the number and the size of encoding packets cached in the MEC server vary for different video files. Therefore, the QoE and transmission latency of each video file are different for the three schemes, which results in different MOS values in the case of the same caching capacity of the MEC server. Furthermore, the MOS values of the Greedy MC-VEB algorithm and MCBST scheme are the same for each video file, because each video file of both schemes is encoded into the minimum encoding rate, and the caching strategy for them is the same when the caching capacity is $\Phi_k = 26880\text{Mb}, \forall k \in \mathcal{K}$, which allows all encoding packets of each video file to be cached in the MEC server at the minimum encoding rate.

B. Average MOS with Different Caching Capacity of MEC server

In Fig. 5, the average MOS value versus different caching capacity of MEC server with $n = 20$, $F = 8$, $K = 1$ is presented. As shown in Fig. 5, the average MOS values of the MC-VEB algorithm and the Greedy MC-VEB algorithm increase with the increasing caching capacity of the MEC server, which eventually tends to the same maximum value determined by the maximum encoding rate of each video file and the optimal caching strategy when the caching capacity of MEC server is sufficient to cache all encoding packets. The MC-VEB algorithm also achieves a considerable performance gain compared with the Greedy MC-VEB algorithm. The minimum average MOS value of the proposed MC-VEB algorithm is obtained when the caching capacity of the MEC server is just enough to cache the minimum number of encoding packets to satisfy the security constraints, while the Greedy MC-VEB algorithm cannot find the feasible solution that satisfies the security constraints at this point, marked by the purple circle in Fig. 5. As the caching capacity of the

TABLE II
MOS OF EACH VIDEO FILE UNDER DIFFERENT CACHING CAPACITY

MOS of Each Video File under the Smallest Caching Capacity								
Index of Video File	1	2	3	4	5	6	7	8
Encoding Rate (Mbps)	0.3	0.3	0.3	0.3	1	1	4	4
Number of Cached Packets	15	19	17	14	18	18	16	15
MOS	3.302	3.303	3.303	3.300	2.984	2.966	2.708	2.695
MOS of Each Video File under the Largest Caching Capacity								
Index of Video File	1	2	3	4	5	6	7	8
Encoding Rate (Mbps)	0.7	0.7	0.7	0.7	4	4	8	8
Number of Cached Packets	20	20	20	20	20	20	20	20
MOS	4.116	4.116	4.116	4.116	3.932	3.932	4.261	4.261

MEC server increases, the gap of the average MOS values first increases, then gradually narrows because that large caching capacity can provide more choices of caching strategy and encoding rate, which could bring better performance on QoE and transmission latency.

Furthermore, the average MOS value of the MCBST scheme, which is always worse than the average MOS value of the proposed MC-VEB algorithm and Greedy MC-VEB algorithm, remains unchanged with the increasing caching capacity. This scenario is reasonable since the minimum encoding rate is adopted in the MCBST scheme, and the caching strategy is the same regardless of the caching capacity because its aim is to minimize the backhaul link rate. As a result, the video encoding packets cached in the MEC server will be as many as possible if the caching capacity is large enough and all encoding packets are cached in the MEC server when each video file is encoded into its minimum encoding rate.

The Greedy MC-VEB algorithm and the MCBST scheme cannot achieve secure transmission when the caching capacity value is very small, i.e., the first point marked by the purple circle in Fig. 5 with caching capacity $\Phi_k = 21540\text{Mb}, \forall k \in \mathcal{K}$, while the proposed MC-VEB algorithm can ensure secure transmission and obtain a feasible average MOS value by adjusting caching strategy and encoding parameters at the same time. The observations above demonstrate the benefits of the proposed algorithms, which comprehensively consider the interaction of caching strategy and encoding parameters.

To show the changes of encoding parameters and caching strategy under different caching capacity, encoding rates and the number of cached packets for two selected points in Fig. 5 are given in Table II. From Fig. 5, at the first point marked by the purple circle, the minimum average MOS value of the proposed MC-VEB algorithm is obtained and at the last point marked by the black circle, the same maximum average MOS values of the proposed MC-VEB algorithm and Greedy MC-VEB algorithm are obtained. Table II gives the MOS value of each video file at the first point when the MEC server has the smallest caching capacity $\Phi_k = 21540\text{Mb}, \forall k \in \mathcal{K}$ and at the last point when the MEC server has the largest caching capacity $\Phi_k = 69660\text{Mb}, \forall k \in \mathcal{K}$. The minimum MOS of each video file is obtained at the first point. In this

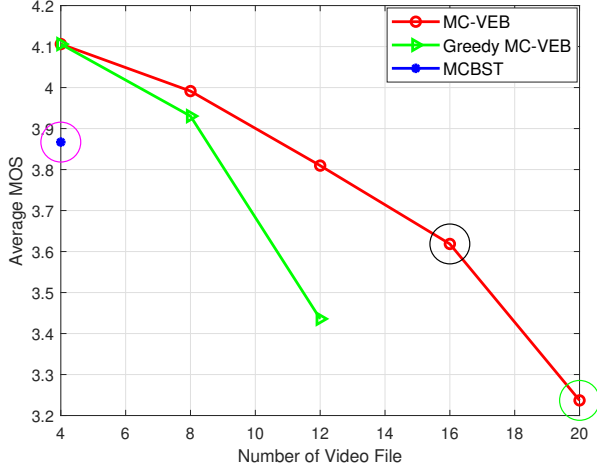


Fig. 6. Average MOS vs. different number of video files

situation, all video files in the MC-VEB algorithm are encoded into the minimum encoding rates, and the minimum number of encoding packets are cached in the MEC server to satisfy the security constraints due to the limited caching capacity. Meanwhile, the minimum number of cached packets varies for different video files, because different video files have a different number of requests. At the last point, the maximum MOS of each video file is obtained, all video files of both algorithms are encoded into the maximum encoding rates, and in both algorithms, all encoding packets are cached in the MEC server due to the sufficient caching capacity.

C. Average MOS with Different Parameters of Video Files

Fig. 6 shows the average MOS value versus different number of video files with $n = 10$, $K = 1$ and $\Phi_k = 39000\text{Mb}, \forall k \in \mathcal{K}$. From Fig. 6, the average MOS value decreases with the increasing number of video files for the proposed MC-VEB algorithm and the Greedy MC-VEB algorithm. The gap between them increases with the increasing video files when the number of video files is less than or equal to $F = 12$. However, the Greedy MC-VEB algorithm has no solution as the number of video files continues to increase to $F = 16$ and $F = 20$, marked by the black and cyan circles in Fig. 6, while the MC-VEB algorithm still has the feasible and effective solution, and the minimum average MOS value is obtained at the last point marked by the cyan circle when all video files are encoded into the minimum encoding rates, and the minimum number of encoding packets are cached in the MEC server.

The reasons contributing to these observations are that when there are four video files, all of them in the two algorithm are encoded into the maximum encoding rates, and all encoding packets are cached in the MEC server due to the sufficient caching capacity, which brings the best MOS values as shown by the first point. As the number of video files increases, only part of the encoding packets can be cached in the MEC server due to the limited caching capacity, which also cannot allow all video files to be encoded into the maximum encoding

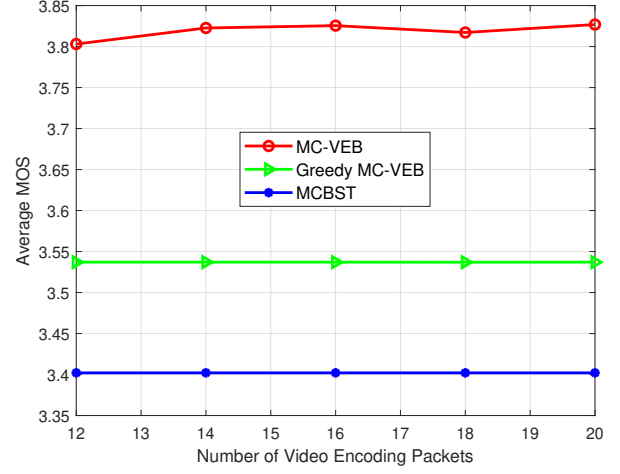


Fig. 7. Average MOS vs. different number of video encoding packets

rates. In this situation, the caching strategy and encoding parameters of the proposed two algorithms are different. For the MC-VEB algorithm, the near optimal average MOS value can be obtained by jointly optimizing the caching strategy and encoding parameters flexibly, while the Greedy MC-VEB algorithm achieves worse MOS values or even an infeasible solution because it optimizes the caching strategy and encoding parameters step by step and thus, cannot satisfy the complex and strict security constraints when there are many video files. This phenomenon further demonstrates the performance advantage of the near optimal MC-VEB algorithm.

Furthermore, it is interesting to find that there is only one feasible point marked by the purple circle in Fig. 6 for the MCBST scheme when there are four video files in the considered scenario, and the performance of its average MOS value is much worse than the proposed algorithms, because when the encoding parameters are fixed, the MCBST scheme cannot satisfy the security constraints by adjusting its caching strategy when there are many video files, and the caching capacity is limited. Meanwhile, the simple caching strategy of the MCBST scheme demands that the number of encoding packets cached in different MEC servers must be the same for the same video file.

In Fig. 7, the average MOS value versus the different number of video encoding packets with $F = 8$, $K = 1$ and $\Phi_k = 28000\text{Mb}, \forall k \in \mathcal{K}$ is presented. From Fig. 7, the average MOS values of the proposed MC-VEB algorithm, Greedy MC-VEB algorithm and the comparable MCBST scheme are almost stable with the increasing number of encoding packets. The MOS performance of the proposed near-optimal MC-VEB algorithm fluctuates slightly when the number of encoding packets changes, which is significantly superior to the Greedy MC-VEB algorithm and the comparable MCBST scheme. Specifically, the MOS performance increases slowly at first, then decreases when the encoding packets increase to $n = 18$, and finally increases to the maximum value when the number of encoding packets is $n = 20$. The fluctuations result from the caching strategy and the encoding parameters

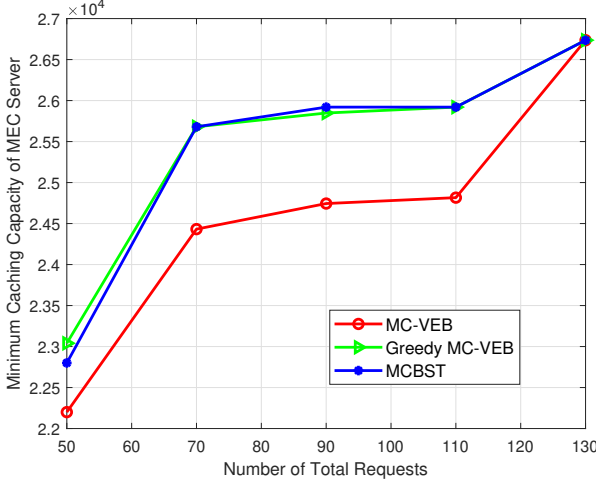


Fig. 8. Minimum caching capacity vs. different number of total requests

varying slightly with the changing total number of encoding packets when the caching capacity and the number of video files remain unchanged. As the number of encoding packets increases, there are more choices of caching strategy to satisfy the security constraints and obtain the better performance of QoE and transmission latency. However, with the increasing number of encoding packets, the size of each encoding packet becomes smaller at the same encoding rate, which could cause the increase in transmission latency. Therefore, the whole performance of the average MOS value cannot change much. A tradeoff exists between the total number of encoding packets and the size of each encoding packet, which results in the falling fluctuation when the number of encoding packets is $n = 18$. In this situation, the proposed near-optimal MC-VEB algorithm will wisely consider this balance and achieve the near-optimal results by joint adjustment of caching strategy and encoding parameters, which also brings the reasonable fluctuations.

As for the Greedy MC-VEB algorithm, its performance of the average MOS value is still better than that of the comparable MCBST scheme, while the average MOS values of both schemes almost remain unchanged when the number of encoding packets changes. This is because that both of them optimize the caching strategy with the fixed encoding parameters, which results in the same caching strategy when the caching capacity of the MEC server and the number of video files keep unchanged in spite of the changing number of total encoding packets. Furthermore, we can find that the gaps of the average MOS values between the proposed MC-VEB algorithm, Greedy MC-VEB algorithm and the comparable MCBST scheme in Fig. 7 are strictly consistent with those of Fig. 5 when the caching capacity of MEC server is $\Phi_k = 28000\text{Mb}, \forall k \in \mathcal{K}$, which further validates the rationality of our simulation results.

D. Average MOS with Different Number of Requests of Users

Fig. 8 shows the minimum caching capacity of the MEC server versus different number of total requests with $n = 10$,

$F = 8$, $K = 1$. The minimum caching capacity of the three schemes increases with the increasing number of total requests and eventually tends to the same value when the number of total requests reaches $\psi = 130$ because, as the number of total requests increases, more caching capacity is needed to cache more video encoding packets to ensure the requirements of QoE, transmission latency and security constraints.

Furthermore, Fig. 8 shows that the the minimum caching capacity of the proposed MC-VEB algorithm is much smaller than the minimum caching capacity of the Greedy MC-VEB algorithm and the comparable MCBST scheme. This phenomenon shows that the proposed MC-VEB algorithm still has relatively good performance even with limited caching resources and can spare more caching resources to achieve better QoE and low latency under the condition of ensuring the security constraints. The minimum caching capacity of the three schemes finally reaches the same value as the number of total requests increases to $\psi = 130$, resulting from more requests indicating that more video encoding packets should be cached in the MEC server for any scheme. As a result, almost all video encoding packets are cached in the MEC server at the minimum encoding rates to satisfy the security constraints and guarantee the QoE and latency requirements when the number of total requests reaches $\psi = 130$.

E. Complexity Analysis

In this subsection, the computational complexity of our proposed MC-VEB algorithm, Greedy MC-VEB algorithm and the MCBST scheme in [33] is analyzed.

(1) MC-VEB: For our proposed near-optimal MC-VEB algorithm, the computational complexity is determined by the GlobalSearch algorithm and 0-1 branch and bound method as shown in Algorithm 1. For the GlobalSearch algorithm, the dimension of the optimization variable is $(K + 1) \cdot n \cdot F$. Then, the computational complexity of the GlobalSearch algorithm can be given by $O(h_g((K + 1) \cdot n \cdot F))$, where $h_g(\cdot)$ is the number of operations positively related to the dimension of the optimization variable. Finally, the computational complexity of the MC-VEB algorithm is $O(h_g((K + 1) \cdot n \cdot F) + N_n \cdot N_b \cdot h_g((K + 1) \cdot n \cdot F))$.

(2) Greedy MC-VEB: As shown in Algorithm 2, the computational complexity of our proposed Greedy MC-VEB algorithm is determined by the Algorithm 1 with a fixed known \mathbf{S} and the optimization algorithm of encoding parameters based on the optimized caching strategy $\tilde{\mathbf{M}}_g$. For Algorithm 1 with a fixed known \mathbf{S} , since the dimension of optimization variable is $K \cdot n \cdot F$, then the computational complexity can be given by $O(h_g(K \cdot n \cdot F))$. Finally, the computational complexity of the Greedy MC-VEB algorithm is $O(h_g(K \cdot n \cdot F) + N_n \cdot N_b \cdot h_g(K \cdot n \cdot F) + N_1 \cdot N_2)$.

(3) MCBST in [33]: For the MCBST scheme, since it only aims to optimize caching strategy without considering video encoding, then the computational complexity is $O(h_g(K \cdot n \cdot F) + N_n \cdot N_b \cdot h_g(K \cdot n \cdot F))$.

Based on the analysis above, compared with the Greedy MC-VEB algorithm, the increase in the dimension of the optimization variable in our proposed near-optimal MC-VEB

algorithm brings higher computational complexity, which has a much greater impact on the running time than the increase in the number of iterations caused by optimizing the encoding parameters alone based on the greedy method. In our simulation, the running time of the near-optimal MC-VEB algorithm is approximately 10^2 times the running time of the Greedy MC-VEB algorithm. For the MCBST scheme in [33], the computational complexity is lower than our Greedy MC-VEB algorithm because the video encoding is not considered. However, as mentioned above, the increase in the number of iterations for optimizing the encoding parameters has a trivial effect on the running time. Therefore, the difference between the computational complexity of the Greedy MC-VEB algorithm and the MCBST scheme in [33] is very small, which can be considered almost the same to some extent.

VIII. CONCLUSIONS

In this paper, we proposed a QoE-driven cross-layer optimization scheme for secure video transmission over the backhaul link in cloud-edge networks. First, we established a video encoding and MEC-caching-based secure transmission model for the backhaul link. Based on the established model, we formulated a joint optimization problem of video encoding parameters and MEC caching strategy to improve user QoE and reduce transmission latency. Then, a near-optimal algorithm based on the relaxation and branch and bound was designed to solve the joint optimization problem. Furthermore, we proposed a greedy algorithm with low complexity to obtain the sub-optimal solution. Simulation results were presented to show that our proposed algorithms can greatly improve QoE and reduce transmission latency under the condition of ensuring secure transmission of the backhaul link compared with the existing algorithm. In addition, our proposed algorithms are proven to be more robust for caching capacity and can ensure secure transmission for more videos with limited caching capacity of MEC servers.

REFERENCES

- [1] Y. Hu, M. Patel, D. Sabella, N. Sprecher, and V. Young, "Mobile edge computing: A key technology towards 5g," *ETSI White Paper*, vol. 11, no. 11, pp. 1-16, 2015.
- [2] N. Abbas, Y. Zhang, A. Taherkordi, and T. Skeie, "Mobile edge computing: A survey," *IEEE Internet of Things J.*, vol. 5, no. 1, pp. 450-465, Feb. 2018.
- [3] X. Chen, L. He, S. Xu, S. Hu, Q. Li, and G. Liu, "Hit ratio driven mobile edge caching scheme for video on demand services," in *Proc. IEEE Int. Conf. Multimedia Expo (ICME)*, Shanghai, China, Jul. 2019, pp. 1702-1707.
- [4] L. Dong, Z. Han, A. P. Petropulu, and H. V. Poor, "Improving wireless physical layer security via cooperating relays," *IEEE Trans. Signal Process.*, vol. 58, no. 3, pp. 1875-1888, Mar. 2010.
- [5] N. Yang, L. Wang, G. Geraci, M. Elkaslan, J. Yuan, and M. D. Renzo, "Safeguarding 5G wireless communication networks using physical layer security," *IEEE Commun. Mag.*, vol. 53, no. 4, pp. 20-27, Apr. 2015.
- [6] Y. Liu, H. Chen, and L. Wang, "Physical layer security for next generation wireless networks: Theory, technologies, and challenges," *IEEE Commun. Surveys Tuts.*, vol. 19, no. 1, pp. 347-376, 1st Quart., 2016.
- [7] J. Chen, L. Yang, and M. Alouini, "Physical layer security for cooperative NOMA systems," *IEEE Trans. Veh. Technol.*, vol. 67, no. 5, pp. 4645-4649, May 2018.
- [8] Y. Mao, C. You, J. Zhang, K. Huang, and K. B. Letaief, "A survey on mobile edge computing: The communication perspective," *IEEE Commun. Surveys Tuts.*, vol. 19, no. 4, pp. 2322-2358, 4th Quart., 2017.
- [9] W. Shi, J. Cao, Q. Zhang, Y. Li, and L. Xu, "Edge computing: Vision and challenges," *IEEE Internet of Things J.*, vol. 3, no. 5, pp. 637-646, Oct. 2016.
- [10] J. Li, Y. Chen, Z. Lin, W. Chen, B. Vucetic, and L. Hanzo, "Distributed caching for data dissemination in the downlink of heterogeneous networks," *IEEE Trans. Commun.*, vol. 63, no. 10, pp. 3553-3568, Oct. 2015.
- [11] A. Sengupta, R. Tandon, and O. Simeone, "Cache aided wireless networks: Tradeoffs between storage and latency," in *Proc. Annu. Conf. Inf. Sci. Syst. (CISS)*, Mar. 2016, pp. 320-325.
- [12] H. Hsu and K. Chen, "A resource allocation perspective on caching to achieve low latency," *IEEE Commun. Lett.*, vol. 20, no. 1, pp. 145-148, Jan. 2016.
- [13] S. Mller, O. Atan, and M. V. D. Schaar, "Context-aware proactive content caching with service differentiation in wireless networks," *IEEE Trans. Wireless Commun.*, vol. 16, no. 2, pp. 1024-1036, Feb. 2017.
- [14] S. Li, J. Xu, M. V. D. Schaar, and W. Li, "Trend-aware video caching through online learning," *IEEE Trans. Multimedia*, vol. 18, no. 12, pp. 2503-2516, Dec. 2016.
- [15] W. Liu, J. Zhang, Z. Liang, L. Peng, and J. Cai, "Content popularity prediction and caching for ICN: A deep learning approach with SDN," *IEEE Access*, vol. 6, pp. 5075-5089, Dec. 2017.
- [16] T. Hou, G. Feng, S. Qin, and W. Jiang, "Proactive content caching by exploiting transfer learning for mobile edge computing," in *Proc. IEEE Glob. Commun. Conf. (GLOBECOM)*, Singapore, Dec. 2017, pp. 1-6.
- [17] Z. Wang, L. Sun, C. Wu, and S. Yang, "Enhancing internet-scale video service deployment using microblog-based prediction," *IEEE Trans. Parallel Distrib. Syst.*, vol. 26, no. 3, pp. 775-785, Mar. 2015.
- [18] Z. Zhang, M. Hua, C. Li, Y. Huang, and L. Yang, "Placement delivery array design via attention-based sequence-to-sequence model with deep neural network," *IEEE Wireless Commun. Lett.*, vol. 8, no. 2, pp. 372-375, Apr. 2019.
- [19] Y. M. Saputra, D. T. Hoang, D. N. Nguyen, E. Dutkiewicz, D. Niyato, and D. I. Kim, "Distributed deep learning at the edge: A novel proactive and cooperative caching framework for mobile edge networks," *IEEE Wireless Commun. Lett.*, vol. 8, no. 4, pp. 1220-1223, Aug. 2019.
- [20] L. Ale, N. Zhang, H. Wu, D. Chen, and T. Han, "Online proactive caching in mobile edge computing using bidirectional deep recurrent neural network," *IEEE Internet of Things J.*, vol. 6, no. 3, pp. 5520-5530, Jun. 2019.
- [21] C. Li, L. Toni, J. Zou, H. Xiong, and P. Frossard, "QoE-driven mobile edge caching placement for adaptive video streaming," *IEEE Trans. Multimedia*, vol. 20, no. 4, pp. 965-984, Apr. 2018.
- [22] X. Huang, L. He, X. Chen, G. Liu, and F. Li, "A more refined mobile edge cache replacement scheme for adaptive video streaming with mutual cooperation in multi-mec servers," in *Proc. IEEE Int. Conf. Multimedia Expo (ICME)*, London, United Kingdom, Jul. 2020, pp. 1-6.
- [23] C. Liang, Y. He, F. Yu, and N. Zhao, "Enhancing QoE-aware wireless edge caching with software-defined wireless networks," *IEEE Trans. Wireless Commun.*, vol. 16, no. 10, pp. 6912-6925, Oct. 2017.
- [24] D. Huang, X. Tao, C. Jiang, S. Cui, and J. Lu, "Trace-driven QoE-aware proactive caching for mobile video streaming in metropolis," *IEEE Wireless Commun.*, vol. 19, no. 1, pp. 62-76, Jan. 2020.
- [25] A. Mehrabi, M. Siekkinen, and A. Y. Jski, "Energy-aware QoE and backhaul traffic optimization in green edge adaptive mobile video streaming," *IEEE Trans. Green Commun. Netw.*, vol. 3, no. 3, pp. 828-839, Sep. 2019.
- [26] A. Sengupta, R. Tandon, and T. C. Clancy, "Fundamental limits of caching with secure delivery," *IEEE Trans. Inf. Forensics Security*, vol. 10, no. 2, pp. 355-370, Feb. 2015.
- [27] Z. A. Hassan and A. Sezgin, "Fundamental limits of caching in d2d networks with secure delivery," in *Proc. IEEE Int. Conf. Commun. Workshops (ICC Wkshps)*, London, U.K., Jun. 2015, pp. 464-469.
- [28] A. A. Zewail and A. Yener, "Device-to-device secure coded caching," *IEEE Trans. Inf. Forensics Security*, vol. 15, pp. 1513-1524, Sep. 2019.
- [29] M. K. Kiskani and H. R. Sadjadpour, "A secure approach for caching contents in wireless ad hoc networks," *IEEE Trans. Veh. Technol.*, vol. 66, no. 11, pp. 10249-10258, Nov. 2017.
- [30] L. Xiao, X. Wan, C. Dai, X. Du, X. Chen, and M. Guizani, "Security in mobile edge caching with reinforcement learning," *IEEE Wireless Commun.*, vol. 25, no. 3, pp. 116-122, Jun. 2018.
- [31] Z. Su, Q. Xu, J. Luo, H. Pu, Y. Peng, and R. Lu, "A secure content caching scheme for disaster backup in fog computing enabled mobile social networks," *IEEE Trans. Ind. Informat.*, vol. 14, no. 10, pp. 4579-4589, Oct. 2018.
- [32] Q. Xu, Z. Su, Q. Zheng, M. Luo, B. Dong, and K. Zhang, "Game theoretical secure caching scheme in multihoming edge computing-enabled heterogeneous networks," *IEEE Internet of Things J.*, vol. 6, no. 3, pp. 4536-4546, Jun. 2019.

- [33] F. Gabry, V. Bioglio, and I. Land, "On edge caching with secrecy constraints," in *Proc. IEEE Int. Conf. Commun. (ICC)*, Kuala Lumpur, Malaysia, May 2016, pp. 1-6.
- [34] M. Zhao, X. Gong, J. Liang, W. Wang, X. Que, and S. Cheng, "QoE-driven cross-layer optimization for wireless dynamic adaptive streaming of scalable videos over HTTP," *IEEE Trans. Circuits Syst. for Video Technol.*, vol. 25, no. 3, pp. 451-465, Mar. 2015.
- [35] V. I. Norkin and G. C. Pflug, "A branch and bound method for stochastic global optimization," *Mathematical programming*, vol. 83, pp. 425-450, Jan. 1998.